

Satellite Attitude Determination Using Magnetometer Data Only

Christin S. Hart¹

United States Air Force Academy, Colorado Springs, Colorado, 80841

On March 8, 2007, the U.S. Air Force Academy launched FalconSAT 3, a complex small satellite with three plasma-researching payloads supporting Department of Defense funded science missions. This is the first three-axis stabilized satellite designed, tested, and built by cadets. FalconSAT 3 is equipped with two types of satellite attitude sensors: magnetometers and sun sensors. However, a software issue inhibits the use of sun sensors, so development of a new method of attitude determination was required. The three-axis magnetometers would need to provide the means to accurately depict the spacecraft's orientation at any given time. Because of the ambiguity involved with using a single form of spacecraft attitude information, Extended Kalman Filtering became a viable solution that would combine insufficient data with a mathematical model of satellite motion to achieve accurate attitude estimation. First, a single-axis Kalman Filter was created for determining the yaw axis, assuming roll and pitch remain zero due to gravity-gradient stabilization. It was found that a constant gain filter can sufficiently provide pointing knowledge, depending on the user's needs. This yaw-estimator also initializes a starting point for a three-axis estimator. Generating a six-state, three-axis control Extended Kalman Filter for attitude determination became the primary focus of research because the FalconSAT 3 payloads require a level of attitude determination accuracy greater than the magnetometers can provide alone. Looking to the future, modification of this three-axis estimator accounts for a pitch wheel considered for FalconSAT 5, a satellite that the U.S. Air Force Academy proposes to launch in December 2009. These three Kalman Filters were developed in England at Surrey Space Centre and were tested and tuned with magnetometer data of a Surrey Satellite Technology Limited (SSTL) satellite called UoSAT. Comparing the attitude estimation results to the truth model of UoSAT shows that the Kalman Filters converge to within one degree of accuracy. This paper details the theory behind these Kalman Filters in addition to their tuning and results.

Nomenclature

F	=	F Matrix relating states to their derivatives
F_1	=	roll-yaw F Matrix [4x4]
F_2	=	pitch F Matrix [2x2]
H	=	observation matrix transforming measurements to desired states
H_1	=	observation matrix for roll-yaw filter [3x4]
H_2	=	observation matrix for pitch filter [3x2]
h	=	pitch wheel angular momentum
K	=	Kalman Gain
K_1	=	Kalman Gain for roll-yaw filter [4x3]
K_2	=	Kalman Gain for pitch filter [2x3]
\bar{P}	=	propagated Covariance
\bar{P}_1	=	roll-yaw propagated Covariance [4x4]
\bar{P}_2	=	pitch propagated Covariance [2x2]
n	=	zero mean measurement noise

¹ FalconSAT 3 ADCS Engineer, U.S. Air Force Academy Small Satellite Research Laboratory, P.O. Box 4305, USAFA CO 80841, AIAA Student Member.

\hat{P}	=	updated Covariance (estimate)
\hat{P}_1	=	roll-yaw updated Covariance [4x4]
\hat{P}_2	=	pitch updated Covariance [2x2]
Φ	=	State Transition Matrix (STM)
Φ_1	=	roll-yaw STM [4x4]
Φ_2	=	pitch STM [2x2]
Q	=	system process noise matrix
Q_1	=	roll-yaw filter system process noise matrix [4x4]
Q_2	=	pitch filter system process noise matrix [2x2]
R	=	system measurement noise [diagonal matrix 3x3]
S	=	Error Deviation Matrix
S_1	=	Error Deviation Matrix for roll-yaw filter [2x2]
		$\sigma_1 = q_1 = q_r$
		$\sigma_3 = q_3 = q_y$
S_2	=	Error Deviation Matrix for roll-yaw filter [constant]
		$\sigma_2 = q_2 = q_p$
\bar{x}	=	propagated state
\bar{x}_1	=	roll-yaw propagated state [4x1]
\bar{x}_2	=	pitch propagated state [2x1]
\hat{x}	=	updated state estimate from $\bar{x}_k = \hat{x}_{k-1} + \int \dot{x} dt$
\hat{x}_1	=	roll-yaw updated state [4x1]
\hat{x}_2	=	pitch updated state [2x1]
\bar{z}	=	reference measurement vector using IGRF (nose-right wing-down frame) [3x1]
\hat{z}	=	calculated or predicted magnetic field measurement vector [3x1]
ϕ	=	roll
θ	=	pitch
ψ	=	yaw
ω_o	=	satellite circular mean motion, a constant
ζ	=	magnetic field measurement in the orbital reference frame taken from Earth's magnetic field model
\bar{b}_{ORF}	=	$\zeta_1 + \zeta_2 + \zeta_3$
B	=	magnetic field measurement in the body frame taken from sensor data

I. Introduction

WHILE working at Surrey Space Centre in conjunction with Surrey Satellite Technology Limited (SSTL), research focused on coding and tuning Extended Kalman Filters for satellite attitude estimation. This work entailed coding Matlab files that produce Euler angles of a spacecraft, given only magnetometer data in the body frame. Euler's Equations of Motion were re-derived to account for the satellite's inertial properties to serve as the mathematical model implemented within the Extended Kalman Filtering programs. The overall project focused on Extended Kalman Filter fundamentals for the FalconSAT Attitude Determination and Control System (ADCS), in which the following Kalman Filters were created:

- Single-axis control linearized Kalman filter for estimating yaw attitude of a gravity gradient-stabilized spacecraft spinning about the yaw axis; results from this filter were used to compare the Kalman Filter versus Constant Gain Filter
- Three-axis control Extended Kalman filter for estimating the attitude of a gravity-gradient stabilized satellite; this flexible filter estimates attitude of axis-symmetric satellites that may or may not include a pitch wheel

II. The Benefits of Kalman Filtering

A Kalman filter is an algorithm that processes corrupted or noisy sensor measurements to more accurately determine a satellite's attitude. When using magnetometers as sensors, the data must be compared to a representation of the Earth's magnetic field, the International Geomagnetic Reference Field (IGRF) model. Unfortunately, the IGRF is an imprecise map of the Earth's magnetic field since the Earth's magnetism is constantly changing due to effects of the sun and irregularities in the atmosphere. Kalman filters can correct for the misrepresentation by converging on the spacecraft's true attitude based on a propagated model embedded in the code.

III. Extended Kalman Filter Fundamentals

The Extended Kalman Filter can be used as a thorough method for updating the Euler angles of the spacecraft, correcting for measurement error through a complex model of propagated states. The Extended Kalman Filter involves non-linearized equations, as opposed to the linear model relating states to their derivatives in a standard Kalman Filter. The attitude estimators discussed in this paper were coded in Matlab because of its powerful matrix capabilities, but any computer language may be used to create Extended Kalman Filters. For a three-axis control Extended Kalman Filter, a state vector holds the information of the current Euler angles and their rates, a total six states. In order to converge on the true attitude of the spacecraft, regardless of imperfect sensor data, the states are propagated forward in time to be compared to the next set of sensor data. The propagated states serve as a model for how the spacecraft attitude is expected to move. Propagation is done with the use of a differential equation of the states, and a rigorous numerical integration method, such as Runge-Kutta 4 (RK4).

The whole idea of a Kalman filter is to minimize error between measured and propagated states: in other words, converge. The difference between the observed states (from satellite sensor data) and propagated states (computed by the Kalman filter) is called the covariance.

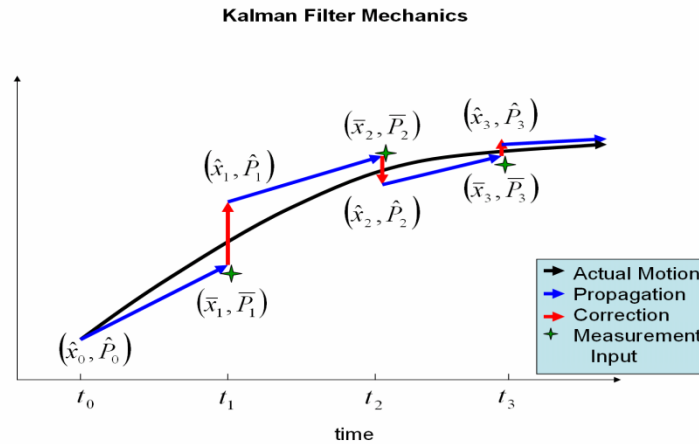


Figure 1. Process of Converging on the True State Vector

Figure 1 shows a visual of how the covariance (in red) is implemented as a correction factor.¹ At each step in the numerical integration process when the states are updated, the covariance is updated, as well. The covariance matrix actually serves as the basis for producing the Kalman gain matrix.

The Kalman gain is the main factor for correcting the propagated states given the covariance information. The gain is necessary for creating accurate propagation and cannot be calculated without the covariance.

IV. Single-axis and Constant Gain Estimators

The first ADCS research project of interest involves a nadir-pointing, gravity gradient-stabilized satellite spinning around the third axis or yaw axis. Hence, the roll and pitch angles are assumed to remain zero, and the yaw angle is rotating 360 degrees over time. The orbit of the axis-symmetric satellite is assumed to be Keplerian and circular.

The axis-symmetric satellite inertia tensor is

$$I = \begin{bmatrix} I & 0 & 0 \\ 0 & I & 0 \\ 0 & 0 & I_3 \end{bmatrix} \text{ assuming } I_3 \ll I \quad (1)$$

Thus, Euler's Equations of motion can be used as governing equations with the gravity-gradient being the only external torque. The purpose of the project was to create an attitude estimator that would determine the spacecraft's yaw angle over time.

The single-axis Extended Kalman Filter was created for three reasons:

- 1) Less complicated than a multi-axis filter and a good exercise for quickly putting to practice the Kalman theory; easier to code and compute the F matrix, etc.
- 2) To seek the feasibility of converting the estimator into a constant gain filter
- 3) For initializing a subsequent three axis estimator by providing the initial yaw condition

A filter with constant gain uses much less processing power than a traditional Kalman filter because the gain does not need to be computed. When an algorithm is looping thousands of times, one less computation saves quite a bit of processing power. And if the constant gain filter meets the spacecraft attitude requirements, it is the most logical and efficient type of filter to use.

The Kalman and Constant Gain single-axis estimators discussed here use two-states: yaw ψ and yaw rate $\dot{\psi}$.

Thus, the state vector is represented by $\bar{x} = \begin{bmatrix} \psi \\ \dot{\psi} \end{bmatrix}$ with a derivative state vector of $\dot{\bar{x}} = \begin{bmatrix} \dot{\psi} \\ \ddot{\psi} \end{bmatrix}$.

Table 1 below represents the actual algorithm for a linearized Kalman Filter, defining (in order) the equations for each matrix or vector.² The symbolic designation as well as a brief description of each matrix or vector is given in addition to the matrix size in the right hand column.

Kalman Filtering Algorithm			
Symbol	Description	Matrix equation	Dimensions
F	Relates states to their derivatives	$\dot{\bar{x}} = F\bar{x}$	[state x state]
Φ	State transition matrix	$\Phi = I + F\Delta t$	[state x state]
\bar{x}	Propagated state matrix	$\bar{x}_k = \hat{x}_{k-1} + \int \dot{\bar{x}} dt$	[state x 1]
\bar{P}	Propagated covariance matrix	$\bar{P}_k = \Phi \hat{P}_{k-1} \Phi^T + Q$	[state x state]
H	Observation matrix	$observed_state = H_k \bar{x}$	[axis det # x state]
K	Kalman Gain matrix	$K_k = \bar{P}_k H_k^T [H_k \bar{P}_k H_k^T + R_k]^{-1}$	[state x axis det #]
\hat{P}	Updated covariance	$\hat{P}_k = [I - K_k H_k] \bar{P}_k$	[state x state]
\hat{x}	Updated state matrix	$\hat{x}_k = \bar{x}_k + K [\bar{z}_k - \hat{z}_k]$	[state x 1]
\bar{z}	Magnetic field intensity reading	$\bar{z}_k = [B_X, B_Y, B_Z]^T$	[3 x 1]
\hat{z}	Calculated magnetic field intensity	$\hat{z}_k = DCM^{Body/ORF} \bar{b}_{ORF_k}$	[3 x 1]

Table 1. Matrix Description, Equation, and Dimension for each step of the Kalman Filtering Algorithm

Because this is a linearized Kalman filter, the F -matrix directly relates the states to their derivatives:

$$F = \begin{bmatrix} 0 & 1 \\ 0 & 0 \end{bmatrix} \quad (2)$$

The z -matrix equations in the last two steps of the above algorithm are shown in detail in the Extended Kalman Filter section.

V. Single-axis and Constant Gain Estimators Results and Validation

Once the Extended Kalman Filter was completed and tuned, the trends of the covariance and Kalman gain matrices were examined in order to come up with a reasonable value of gain that could be held constant: $[0.1, 0.001]^T$. Surrey Space Technology Limited (SSTL) provided a data file to feed into the constant gain filter: six hours of magnetometer BX, BY, BZ with measurements given every four seconds and the true yaw angle in degrees. These 5400 points of data were accompanied by the corresponding Two-Line Element (TLE) sets that were also fed into the estimators. Given the true yaw by SSTL, at each time step, a comparison could be made between the yaw angle produced by the estimator and the true yaw. In real life (as opposed to this simulation) true yaw would not actually be available, but for simulation purposes of testing the estimator, using the true yaw to find filter error produces the following plots shown in *Figure 2*.

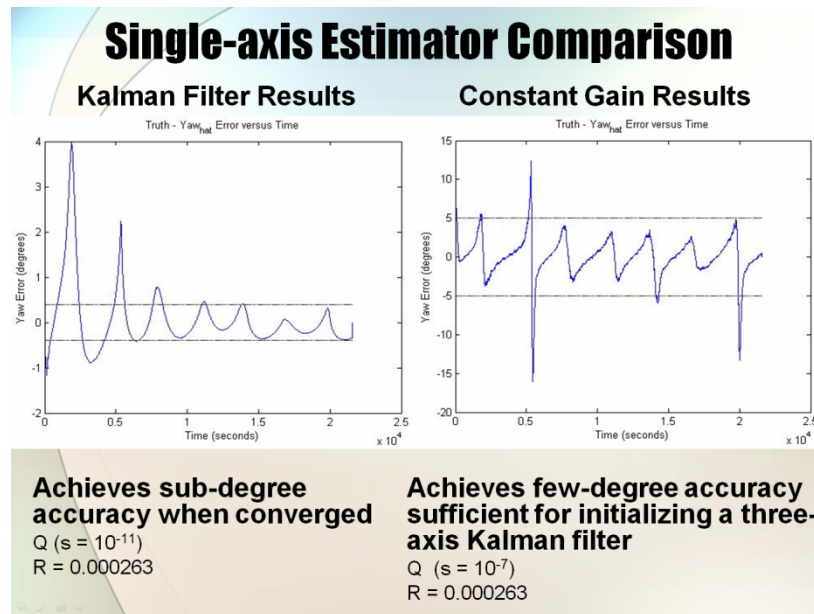


Figure 2. Single-Axis Kalman and Constant Gain Results

The single-axis Extended Kalman Filter and constant gain filter were not created with the expectation of great accuracy; this is because assuming zero pitch and zero yaw is an extreme oversimplification. Nevertheless, the plots above demonstrate both filters converging within roughly ± 15 degrees accuracy. The Extended Kalman Filter produces better accuracy (less than 1 degree), but the constant gain filter uses less processing power. Choosing the best filter for a given mission depends on the client's needs. The FalconSAT 3 mission requires ± 5 degrees of pointing knowledge, depicted on the plots. Because attitude determination for FalconSAT 3 will be post-processed on the ground, meaning computer processing power is not an issue, the more accurate single-axis Extended Kalman Filter will be used.

Before such accuracy could be achieved using these two filters, the system process noise, Q , and system measurement noise matrix, R , were adjusted until the quickest and most accurate convergence occurred. Using more significant values for system measurement noise causes the filter to rely more heavily on the system process or equation model due to such noisy measurement data. A small value for the system process noise applies more weighting on the system data measurements, as is the case in these two filters. For both the Extended Kalman Filter and constant gain filter, the single-celled system measurement noise matrix, R , became 0.000263 as denoted in *Figure 2* above. In addition, the 2x2 system process noise matrix, Q , is the same for both filters: the calculation for Q involves an s term representing error deviation. In optimizing the balance between Q and R , first Q is held constant and then R is manipulated. With the s value for Q set at 10^{-11} , the error between true yaw and estimated yaw was already less than 5 degrees.

The SSTL technique of making a series of array calculations aided in tuning R . The following two equations were used to create two arrays to aid in tuning the filter. At each data step, the values were calculated in these equations to make the arrays.

$$\text{Tuning array 1} = \frac{\zeta_1}{\zeta_2 B_x - \zeta_1 B_y} \quad (3)$$

$$\text{Tuning array 2} = \frac{\zeta_2}{\zeta_2 B_x - \zeta_1 B_y} \quad (4)$$

where \bar{b}_{ORF} is referenced from the IGRF model of the Earth's magnetic field.

$$\bar{b}_{ORF} = \zeta_1 + \zeta_2 + \zeta_3 \quad (5)$$

and B_x, B_y, B_z are magnetic field measurements taken in the three axes of the body frame (provided by SSTL).

The average value of each array was then calculated. Next, the two average array values were multiplied by the magnetic field measurement error for the system magnetometers. For SSTL's UoSAT, the magnetic field measurement error was 0.1 microTesla. By adding these two products and taking the square root of that sum, an incredible estimate for R was made. After two iterations of using the filter to run the results and implementing these tuning calculations, R converged to 0.0002630959654 and the error between true and estimated yaw improved to the order of +/- 0.0530 degrees.

VI. Three-axis Extended Kalman Filter

The next step in the research involved creating an attitude estimator to be implemented on FalconSAT 3, and one that could be potentially modified for FalconSATs 4 and 5. This is a six-state Extended Kalman Filter that computes roll ϕ , pitch θ , yaw ψ , and their respective derivatives roll rate $\dot{\phi}$, pitch rate $\dot{\theta}$, and yaw rate $\dot{\psi}$. The scenario is the same as before: a gravity-gradient stabilized, axisymmetric small satellite in a Keplerian, circular orbit. However, now small pitch and roll are more correctly assumed (instead of zero pitch and roll). Moreover, a pitch wheel is added into the dynamics of the satellite. This is a wheel aligned with the spacecraft's y-body axis that can spin up to control the spacecraft or counteract external torques about the pitch axis.

The first and foremost reason for completing this project was to test the post-processing attitude determination techniques developed for the FalconSAT Program. But, the Extended Kalman Filter also needed to account for pitch wheel dynamics for future satellites of the FalconSAT Program. This involved re-deriving the Euler's Moment Equations with angular momentum of the pitch wheel accounted for in the y-axis direction, shown here:

$$\begin{aligned} 0 &= I\ddot{\phi} + [4\omega_o^2(I - I_3) - \omega_o h]\dot{\phi} - (I_3\omega_o + h)\dot{\psi} \\ 0 &= I\ddot{\theta} + 3\omega_o^2(I - I_3)\dot{\theta} + \dot{h} \\ 0 &= I_3\ddot{\psi} - \omega_o h\dot{\psi} + (I_3\omega_o + h)\dot{\phi} \end{aligned} \quad (6-8)$$

where ω_o denotes satellite circular mean motion, a constant. Letting $k = I_3/I$, and rearranging for the double-derivatives yields the following matrix equation:

$$\begin{bmatrix} \ddot{\phi} \\ \ddot{\theta} \\ \ddot{\psi} \end{bmatrix} = \begin{bmatrix} \left(-4\omega_o^2(1-k) + \frac{\omega_o h}{I}\right)\dot{\phi} + \left(k\omega_o + \frac{h}{I}\right)\dot{\psi} \\ -3\omega_o^2(1-k)\dot{\theta} - \frac{\dot{h}}{I} \\ \left(\frac{\omega_o h}{I_3}\right)\dot{\psi} - \left(\omega_o + \frac{h}{I_3}\right)\dot{\phi} \end{bmatrix} \quad (9)$$

At the same time, because FalconSAT 3 does not have a pitch wheel, this algorithm needed to be able to estimate the spacecraft attitude as usual without a pitch wheel. Thus, the filter was coded so that when zero was entered for pitch wheel angular momentum, h , and rate, \dot{h} the Extended Kalman Filter runs as if no pitch wheel existed.

The following algorithm describes the method of coding this Extended Kalman Filter.² Notice that the pitch equation is decoupled from the roll and yaw equations. Thus, the six states for this Extended Kalman filter can be broken into two state vectors: roll-yaw x_1 and pitch x_2 .

$$x_1 = \begin{bmatrix} \phi \\ \psi \\ \dot{\phi} \\ \dot{\psi} \end{bmatrix} \quad \dot{x}_1 = \begin{bmatrix} \dot{\phi} \\ \dot{\psi} \\ \ddot{\phi} \\ \ddot{\psi} \end{bmatrix} \quad x_2 = \begin{bmatrix} \theta \\ \dot{\theta} \end{bmatrix} \quad \dot{x}_2 = \begin{bmatrix} \dot{\theta} \\ \ddot{\theta} \end{bmatrix} \quad (10-13)$$

The roll-yaw F_1 -matrix is linear, yet roll requires a second f_2 -matrix to complete the mathematical model with the governing equation

$$x = Fx + fh \quad (14)$$

$$F_1 = \begin{bmatrix} 0 & 0 & 1 & 0 \\ 0 & 0 & 0 & 1 \\ -4(1-k)\omega_o^2 + \frac{\omega_o h}{I} & 0 & 0 & k\omega_o + \frac{h}{I} \\ 0 & \frac{\omega_o h}{I_3} & -\omega_o - \frac{h}{I_3} & 0 \end{bmatrix} \quad (15)$$

$$F_2 = \begin{bmatrix} 0 & 1 \\ -3(1-k)\omega_o^2 & 0 \end{bmatrix} \quad f_2 = \begin{bmatrix} 0 & 0 \\ 0 & \frac{-1}{I} \end{bmatrix} \quad (16-17)$$

The system process noise matrix is defined as follows for roll-yaw and pitch, respectively.

$$Q_1 = \begin{bmatrix} q_r^2 \frac{\Delta t^3}{3} & 0 & q_r^2 \frac{\Delta t^2}{2} & -\omega_o q_r^2 \frac{\Delta t^3}{3} \\ 0 & q_y^2 \frac{\Delta t^3}{3} & k\omega_o q_y^2 \frac{\Delta t^3}{3} & q_y^2 \frac{\Delta t^2}{2} \\ q_r^2 \frac{\Delta t^2}{2} & k\omega_o q_y^2 \frac{\Delta t^3}{3} & q_r^2 \Delta t + k^2 \omega_o^2 q_y^2 \frac{\Delta t^3}{3} & k\omega_o q_y^2 \frac{\Delta t^2}{2} - \omega_o q_r^2 \frac{\Delta t^2}{2} \\ -\omega_o q_r^2 \frac{\Delta t^3}{3} & q_y^2 \frac{\Delta t^2}{2} & k\omega_o q_y^2 \frac{\Delta t^2}{2} - \omega_o q_r^2 \frac{\Delta t^2}{2} & q_y^2 \Delta t + \omega_o^2 q_r^2 \frac{\Delta t^3}{3} \end{bmatrix} \quad (18)$$

$$Q_2 = \begin{bmatrix} q_p^2 \frac{\Delta t^3}{3} & q_p^2 \frac{\Delta t^2}{2} \\ q_p^2 \frac{\Delta t^2}{2} & q_p^2 \Delta t \end{bmatrix} \quad (19)$$

The system measurement noise matrix is a single matrix of three dimensions corresponding to the three-axes of attitude determination.

$$R = \begin{bmatrix} R & 0 & 0 \\ 0 & R & 0 \\ 0 & 0 & R \end{bmatrix} \quad (20)$$

The first order propagation of the state-transition matrix, which only varies with change in time step in this case, is

$$\Phi = I + F\Delta t \quad (21)$$

State propagation is performed using RK4 numerical integration. The subscript k represents each iterative step along the way to filter convergence.

$$\bar{x}_k = \hat{x}_{k-1} + \int \dot{x} dt \quad (22)$$

Covariance is propagated using the system process noise matrix.

$$\bar{P}_k = \Phi \hat{P}_{k-1} \Phi^T + Q \quad (23)$$

The magnetic field measurement in the orbital reference frame is taken from the IGRF model using SGP4 propagator.

$$\bar{b}_{ORF} = \bar{z}_k = \begin{bmatrix} \zeta_1 \\ \zeta_2 \\ \zeta_3 \end{bmatrix} \quad (24)$$

The observation matrix relating the observed states to the states of Euler angles and rates is calculated using these orbital reference frame measurements.

$$H_{k1} = \begin{bmatrix} \zeta_3 \sin \psi & -\zeta_1 \sin \psi + \zeta_2 \cos \psi + \zeta_3 (\theta \sin \psi + \phi \cos \psi) & 0 & 0 \\ \zeta_3 \cos \psi & -\zeta_1 \cos \psi - \zeta_2 \sin \psi + \zeta_3 (\theta \cos \psi - \phi \sin \psi) & 0 & 0 \\ -\zeta_2 & 0 & 0 & 0 \end{bmatrix} \quad (25)$$

$$H_{k2} = \begin{bmatrix} -\zeta_3 \cos \psi & 0 \\ \zeta_3 \sin \psi & 0 \\ \zeta_1 & 0 \end{bmatrix} \quad (26)$$

The Kalman gain supplies the necessary correction for properly updating the propagated covariance. The Kalman gain, allows the Extended Kalman Filter to converge on true attitude more quickly than otherwise possible.

$$K_k = \bar{P}_k H_k^T [H_k \bar{P}_k H_k^T + R_k]^{-1} \quad (27)$$

The covariance must be updated before the next iteration of propagation occurs. In this way, the Extended Kalman Filter begins to gain knowledge as it “learns” the satellite attitude situation.

$$\hat{P}_k = [I - K_k H_k] \bar{P}_k \quad (28)$$

In order to also update the actual six states, the difference between observed and predicted magnetic field measurements must be implemented. The predicted z -matrix, \hat{z} , is calculated by

$$\hat{z}^I = T_{R2B} \bar{z}^{TND} + \bar{n} \quad (29)$$

where T_{R2B} is a Directions Cosines Matrix in the Euler 2-1-3 Sequence modeled in the problem.

$$T_{R2B} = \begin{bmatrix} \cos\psi \cos\theta + \sin\psi \sin\phi \sin\theta & \sin\psi \cos\phi & -\cos\psi \sin\theta + \sin\psi \sin\phi \cos\theta \\ -\sin\psi \cos\theta + \cos\psi \sin\phi \sin\theta & \cos\psi \cos\phi & \sin\psi \sin\theta + \cos\psi \sin\phi \cos\theta \\ \cos\phi \sin\theta & -\sin\phi & \cos\phi \cos\theta \end{bmatrix} \quad (30)$$

When small pitch and roll are assumed, the transformation matrix becomes

$$T_{R2B} = \begin{bmatrix} \cos\psi & \sin\psi & -\theta \cos\psi + \phi \sin\psi \\ -\sin\psi & \cos\psi & \theta \sin\psi + \phi \cos\psi \\ \theta & -\phi & 1 \end{bmatrix} \quad (31)$$

(It is incorrect to assume small yaw; the spacecraft is nadir pointing spinning about the the yaw axis.) Using equation 29, the calculated \hat{z} matrix becomes

$$\hat{z}_k = \begin{bmatrix} \zeta_1 \cos\psi + \zeta_2 \sin\psi + \zeta_3(-\theta \cos\psi + \phi \sin\psi) + n_1 \\ -\zeta_1 \sin\psi + \zeta_2 \cos\psi + \zeta_3(\theta \sin\psi + \phi \cos\psi) + n_2 \\ \zeta_1 \theta - \zeta_2 \phi + \zeta_3 + n_3 \end{bmatrix} \quad (32)$$

where the n_i signifies a zero mean measurement noise vector component.

Now, knowing the observed and calculated z -matrices, the six states can be updated.

$$\hat{x}_k = \bar{x}_k + K[\bar{z}_k - \hat{z}_k] \quad (33)$$

Next, state propagation commences again since the F -matrix is constant in this case. The algorithm continues until the Extended Kalman Filter converges with accurate state computations.

VII. Extended Kalman Filter Results and Validation

In order to ensure the Extended Kalman Filter converges accurately, the results are compared to a truth model that represents the spacecraft's actual motion. The same SSTL UoSAT data file used for the first Kalman filter was used to test the Extended Kalman filter; the data includes the three-axes magnetometer measurements in the body frame, time, and true states. The Extended Kalman Filter acts as an attitude estimator, producing Euler angles and their rates at each time step through the iterative process. An Extended Kalman Filter can be considered properly tuned if the Euler angles converge within user-specified range of the true spacecraft attitude. Specifically, the estimated attitude and true attitude adequately match when the error between them becomes zero.

A. Validation with Euler Angle Error

Before conducting this analysis, a model of the true attitude is emulated by using exact attitude equations for a gravity-gradient stabilized spacecraft. The truth model is precisely calculated, unlike the Extended Kalman Filter, which originates from approximated, linearized attitude equations. External torques such as drag and solar pressure are ignored when creating the truth model since the gravity-gradient external torques dominate the scenario. A widely used numerical integration scheme, namely RKF45, rigorously propagates the true attitude. No white

Gaussian noise is added to the truth simulation to maintain pure attitude data. Euler angles are outputted from the truth model in a 2-1-3 direction cosine matrix sequence to coincide with the Extended Kalman Filter design. The truth model is the numerically simulated attitude state that can be regarded as the actual spacecraft Euler angles: true roll, pitch, and yaw.

The Extended Kalman Filter results are analyzed graphically with respect to the truth. The difference between the estimated Euler angles and true Euler angles represents the error. This error is computed separately for roll, pitch, and yaw at each time step in the Extended Kalman Filter. The following plots for roll error, pitch error, and yaw error versus time demonstrate that the Extended Kalman Filter converges upon the true attitude.

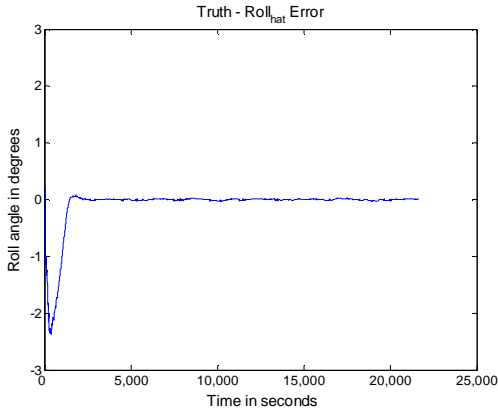


Figure 3. Error between Kalman and True Roll

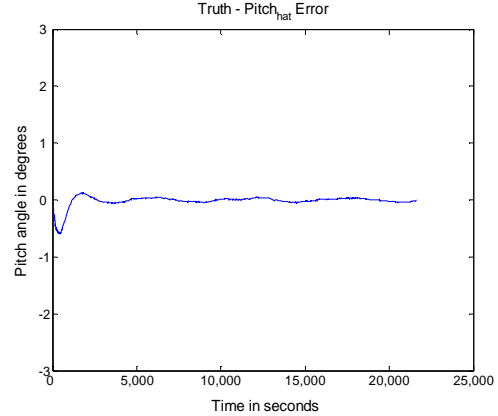


Figure 4. Error between Kalman and True Pitch

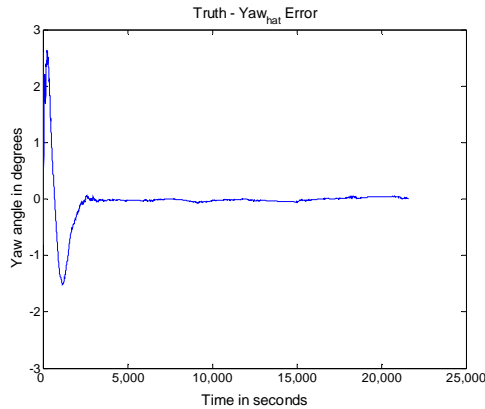


Figure 5. Error between Kalman Yaw and True Yaw

B. Validation with Magnetic Field Error

Another method for verifying the Extended Kalman Filter involves examining the magnetic field strength. The Extended Kalman Filter employs both an observed and a calculated magnetic field strength vector. The observed B-field vector, \bar{z} , taken from the IGRF model represents the magnetic field measurements in the spacecraft's orbital reference frame, otherwise known as \bar{b}_{ORF} . The calculated B-field vector, \hat{z} , equation is shown in the Extended Kalman Filter algorithm above.

Graphing the error between the calculated and observed B-field vector components versus time yields three periodic plots. An example of such a plot is shown below. All three plots appear similar.

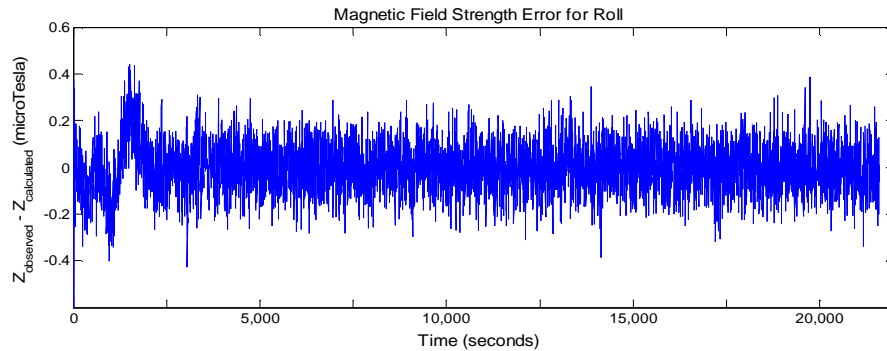


Figure 6. Difference in Observed Roll and Calculated Roll

A sinusoidal pattern in the observed minus calculated plot of the spacecraft Euler angles confirms that the Extended Kalman Filter is working properly.

VII. Conclusion

While in Surrey, mastering the fundamentals of using filters as estimators led to excellent attitude determination. The pros and cons of using Extended Kalman Filtering versus constant gain filtering were explored. The biggest accomplishment was coding a working three-axis Extended Kalman Filter for attitude determination with gravity-gradient stabilized satellites, such as FalconSAT 3. This three-axis estimator exceeds the attitude determination mission requirements for FalconSAT 3. The single-axis Extended Kalman filter also exceeds attitude determination requirements and will, therefore, be used to set FalconSAT 3's yaw-value as the initial condition for the three-axis estimator. The three-axis estimator can effectively provide attitude determination for FalconSAT 3 and future FalconSATs involving pitch-wheel dynamics. The research conducted in Surrey also set the stage for expanding upon the six-state filter for a more complex situation.

Acknowledgments

I would like to thank Dr. Yoshi Hashida for teaching me Extended Kalman Filter coding at SSTL and for developing such fantastic Extended Kalman Filtering doctrine as the small-satellites world expert on ADCS.

Thank you to Dr. Paul Vergez for encouraging me by being an amazing mentor and role model.

Thank you, Col France, for giving me the opportunity to research in Surrey, England and to write two AIAA student papers.

Thank you, Lt Col Timothy Lawrence, for your support in the Cadet Summer Research Program.

I would also like to thank my predecessors, 2nd Lts. Robert Bethancourt and Christopher Taylor, for preparing me for summer research. Without the background they gave me, I would have been off to an arduous start.

Thanks to my ADCS colleagues, Todd Small and Gavin McCorry, for working with me to continue the FalconSAT Program ADCS task to the next generation.

References

¹Hale, M. J., Vergez, P., and Meerman, M. J., "Kalman Filtering and the Attitude Determination and Control Task," AIAA-2004-6018, U.S. Air Force Academy Department of Astronautics, Colorado Springs, Colorado, September 2004.

²Hashida, Y., "ADCS for Future UoSat Standard Platform: Revision 2," Surrey Satellite Technology Limited, Guildford, UK, August 2004.